Journal of New Results in Science (JNRS)
*ISSN: 1304-7981*
*http://dergipark.gov.tr/en/pub/jnrs*
*Research Article*
*Open Access*

**Volume:** 9
**Issue:** 2
**Year:** 2020
**Pages:** 17-31

***Received***: 26.06.2020 ***Accepted***: 02.09.2020

# Experimental and Theoretical Approaches for the Characterization of the Novel ((Ethane-1,2-diylbis(azanediyl))bis(carbonyl))bis(4,1-phenylene) Diacrylate Molecule

**Uğur, SOYKAN[a,*] , Sedat CETİN[b], Gürcan YILDIRIM[c]**

*[a]Yeniçağa Yaşar Çelik Vocational High School, Bolu Abant Izzet Baysal University, Bolu, Turkey.*
*[b]Department of Chemistry, Faculty of Arts and Sciences, Bolu Abant Izzet Baysal University, Bolu, Turkey.*
*[c]Department of Mechanical Engineering, Faculty of Engineering, Bolu Abant Izzet Baysal University, Bolu, Turkey.*
**Corresponding author e-mail, ugursoykan@ibu.edu.tr*

**ABSTRACT:** This multidisciplinary study deals with not only the synthesis of the novel ((ethane-1,2-diylbis(azanediyl))bis(carbonyl))bis(4,1-phenylene) diacrylate (ABCEDA) molecule but also the experimental and theoretical (with DFT and HF methods) characterization of the title compound for the first time. The experimental results obtained from FT-IR and $^1$H-NMR verified that the title novel molecule was synthesized without any impurities and the reaction yield was about 68 wt%. DSC melting temperature and crystallization temperature belonging to the studied molecule were found to be 335 °C and 226 °C, respectively. As for molecular geometric properties, there was little deviation on the calculated bond angles and bond lengths of the compound. Both bond angles and bond lengths computed from DFT method were slightly greater than the results obtained from the HF method due to the fact that the electron correlation coefficients were taken into account in DFT method. The optical band gap energy of the compound was computed to be about 0.3904 a.u. (10.6233 eV), conforming that the molecule had low electronic donor ability. Moreover, MEP analysis showed that the molecule possessed the possible sites for the electrophilic and nucleophilic attacks. Furthermore, the negative ESP spread over mostly on the oxygen atom whereas the positive ESP was located on the rest of the molecule.

***Keywords:****((ethane-1,2-diylbis(azanediyl))bis(carbonyl))bis(4,1-phenylene) diacrylate, DFT/HF methods, molecular geometry, HOMO-LUMO, MEP-ESP maps.*

## 1. Introduction

The term of cross-linking agent describes as a material including two or more reactive and specific functional ends having capable of reacting with another polymer molecules. That is, two polymer chains join together by means of a branch referred to as a crosslink. The most widely used cross-linkers in the literature are divinylbenzene (Yin et al., 2015),ethyleneglycol dimethacrylate (Philip and Mathew, 2008), N,N' methylene bisacrylamide (Zhao et al, 2008), 1,4-phenylene diacrylamide (Cormack and Elorza, 2004), tetramethylene dimethacrylate (Stankova et al, 2013). Synthetic cross-linker having various functional groups and different chain lengths were also synthesized (Gomez and Strumia, 2001; Zhan et al, 2018). It is well-known that the cross-linking agents are extremely essential for the development in the material engineering and commercial standpoint (Elder et al, 2011; Gao et al, 2012; Martinez et al, 2015). Especially, the polymeric materials having desired characteristics are produced with the use of cross-linking agents bearing polyfunctional groups in their structure. That is, they impart the excellent stability toward physical stress and elevated temperatures to the polymeric materials (Abdelkader and White, 2005; Zhang et al, 2015). Moreover, the cross-linked polymers gain the dimensionally stability under a wide variety of conditions due to the forming rigid network structure (Montazer and Jolaei, 2010). Such polymers are described as the thermosetting polymers having non-flowing behavior with irreversibly hardened feature due to the cross-linked network. The structural integrity and chemical resistance are high in the thermosetting polymer and they also have the improving mechanical properties due to showing the resistance to deformation (Pittman et al, 2000). In addition to that, the cross-linkers are commonly used for the preparation of polymer gels which are swollen in the solvent without dissolving (Luo et al, 2011). Polymer gel with unique physiochemical properties have attracted much attention in polymer science (Osada et al, 2004). By cross-linking, the polymer gels possessed swellable network structures, which having ability to give response to change in electric field (Pascal et al, 2019), solvent composition (Lenhart and Cole, 2006), acidity (Iwakura et al., 2001) and temperature (Maryanski et al, 1997). Furthermore, the bead polymers could be produced by using cross-linkers under the proper synthesis condition. The crosslinker characteristics during the preparation of cross-linked microspheres affect the mechanical strength, insolubility, stiffness, rigidity, shape and particle size of the microspheres (Margel et al, 1991; Park et al, 2003.) Shortly, it is clear that the cross-linkers have had a important role in the modern polymer science.

On the other hand, there existed lots of theoretical studies focusing on the determination of electrical, structural and dynamic phenomenon of both a molecule and cross-linked polymers to obtain effective and reliable results in the short time (Benhamou and Chahid, 2008; Benmouna et al, 2001; Karaboga et al., 2013; Sert et al., 2019; Smolin et al, 2017). In other words, some crucial features and experiment phenomena of the compounds can be elucidated effectively by means of the proper quantum theoretical methods (Sun et al, 2010). Density functional theory (DFT) and ab initio Hartree Fock (HF) have large popularity in the present theoretical world. They provide us with effective theoretical approach procedures in order to examine the structural, physical, optical and electrical properties of the novel synthesized molecules. Of these theoretical methods, some researchers exhibited that DFT methods gives better results than those of the HF ones (Cirak and Koc, 2012; Gokce and Bahceli, 2011; Ucun et al, 2008). The electronic energy is treated as a function of electron density of all electrons in the former theoretical methods and electron correlation effects are not taken consideration at HF method. Conversely, DFT method recovers the electron correlation along with the density function of electrons, which make it more reliable and effective when compared to other theoretical methods (Cirak and Koc, 2012; Durig et al, 2011).

In the current paper, we studied not only the synthesis of the novel title molecule from cross-linking agent family and the identification by theoretical and experimental investigations. Fourier transformation-infrared (FTIR) spectra, differential scanning colorimeter (DSC) thermogram and nuclear magnetic resonance (NMR) chemical shift measurements were conducted for the experimental examinations. The optimized molecular structure, bond lengths and bond angles were determined by means of both density functional theory (B3LYP) and Hartree Fock (HF) with the standard 6-31G(d,p) calculation level. The electronic properties (HOMO, LUMO, electronegativity, chemical hardness, softness, electrophilic index, electrostatic potential) are also investigated in details with density functional theory (B3LYP) with the standard 6-31G(d,p) calculation level. All the obtained results were discussed meticulously.

## 2. Material and Methods

### 2.1. Materials

For the synthesis of the novel crosslinking agent (ABCEDA), the main chemicals, acryloyl chloride (AC), p-hydroxybenzoic acid (HBA), thionyl chloride (Merck A.G.), ethylenediamine (EDA) were purchased form Merck A.G. and they were used as received form the campany. All the other solvents and chemical being analytical grade were used without any purification processes.

## 2.2. Instruments

FT-IR analysis of the synthesized novel cross-linking agent, ABCEDA were conducted by a Shimadzu 8400 S FTIR spectrophotometer in the region 400-4000 cm$^{-1}$. KBr pellets containing roughly 3 mg of sample in 100 mg spectroscopic grade KBr were prepared for obtaining FTIR spectra. JEOL-ECS 400 $^1$H-NMR spectra of the ABCEDA was performed with a frequency of 400 MHz in deuterated chloroform ($CDCl_3$) with the use of tetramethylsilane (TMS) as an internal reference in parts per million (ppm) scales. The thermal analysis of the obtained products was conducted by Shimadzu TA-60 WS Differential Scanning Calorimeter under nitrogen atmosphere with a heating rate of 10°C/min and the amount of sample changed between 5-15 mg.

## 2.3. Synthesis of ABCEDA

The novel diacrylate compound, ABCEDA was prepared by condensation reaction between ethylenediamine and p-acryloyloxybenzoyl chloride (ABC). The synthesis of ABC and p-acryloyloxybenzoic acid (ABA) were announced in our previous study in detail (Soykan et al., 2013). 9.5 mmol of ABC prepared was dissolved in 100 mL of acetone in a flask equipped with a magnetic stirrer. 100 mL of acetone solution containing 4.75 mmol of ethylenediamine, 9.50 mmol of triethylamine and catalytic amount of pyridine was added dropwise to ABC solution at room temperature for 24 hours. After the reaction complete, white triethylamine hydrochloride salt formed during the reaction was extracted from the product by successive washings with water (3-4 times). The remaining water in solution was removed by using drying agent ($Na_2SO_4$) and then filtered off. Finally, the solvent was evaporated, and the product was dried in vacuum at room temperature. The reaction yield was found to be about 68 wt% and the simplified reaction steps were displayed in Figure 1. The characterization of the novel cross-linking agent, ABCEDA was done by means of FTIR, DSC and $^1$H-NMR techniques.

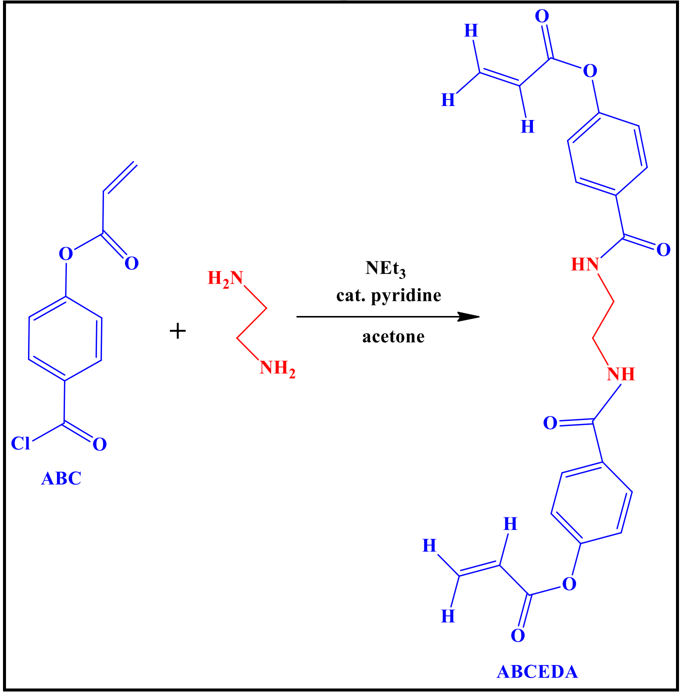

**Fig. 1.** The simplified demonstration of the reaction steps for the synthesis of ABCEDA

### 2.4. Computational details

Optimized molecular structure, bond lengths and bond angles of the new title compound were determined for the first time by using Gaussian 09 package program with the molecular visualization program by means of both B3LYP (Stephens et al, 1994) and Hartree Fock (HF) (Ceylan et al, 2016) methods at 6-31G(d,p) calculation level. The results obtained from both methods were discussed in detail. Furthermore, the determination of electronic properties of the title compound was only carried out at B3LYP with the standard 6-31G(d,p) (Akyildiz et al, 2018; Arioglu et al, 2018) calculation level since electron correlation were taken into account in the calculations.

## 3. Results and Discussion

### 3.1. Characterization of ABCEDA

The FTIR spectrum of ABCEDA bearing double amide, ester, phenyl and acrylic groups in their structure was depicted in Figure 2. The moderate absorption peaks observed at 3325 cm$^{-1}$ is due to N-H stretching vibrations of amide groups. The IR bands designated at about 3070 cm$^{-1}$ and at about 2939 cm$^{-1}$ are assigned to aromatic stretching vibrations of C-H bond in the phenyl groups and the stretching vibrations of CH$_2$ bonds, respectively. The strong band at 1735 cm$^{-1}$ is attributed to the C=O stretching vibrations of the ester groups and the bands detected at 1631 cm$^{-1}$ is due to the stretching vibrations of C=C bonds in the vinylic groups. The strong bands detected at 1539 cm$^{-1}$ is corresponding to C=O stretching vibrations of the amide groups. The absorption band assigned to aromatic stretching vibrations of C=C bonds is found to be in the range of 1500-1604 cm$^{-1}$. The strong bands observed at 1203 cm$^{-1}$ and 1172 cm$^{-1}$ are due to C-O and C-N bonds in the structure, respectively. The moderate bands appearing between 806 and 1018 cm$^{-1}$ represent the vinylic C-H out-of-plane bending vibrations.

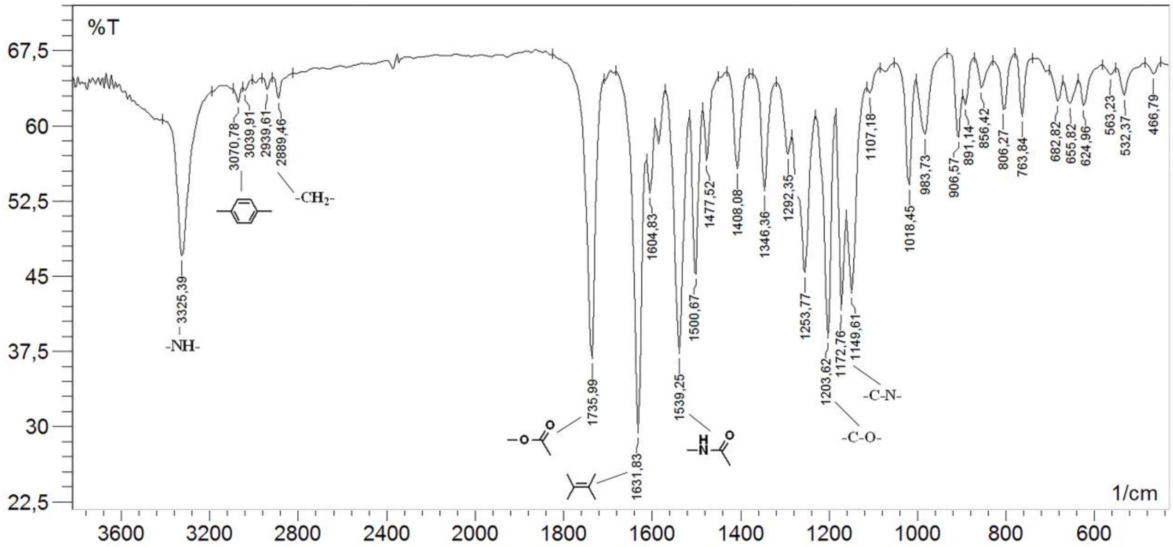

**Fig. 2.** FTIR spectrum of the ABCEDA

$^{1}$H-NMR spectra belonging to the ABCEDA crosslinking agent is displayed in Figure 3. It is visible from the figure that three doublets at about δ 6.0, 6.3 and 6,6 are corresponding to Hb, Ha and trans coupling of Hc protons of vinylic groups, respectively. Hd and He protons which correspond single O-coupling of the -$C_6H_4$ groups in the structure gives two multiplet peaks at δ 7.2 and 7.8, respectively. In addition, the broad singlet at δ 7.0 is attributed to Hg protons of N-H groups. The one triplet at δ 3.7 is clearly corresponding to Hf protons of -$CH_2$ groups in molecule.

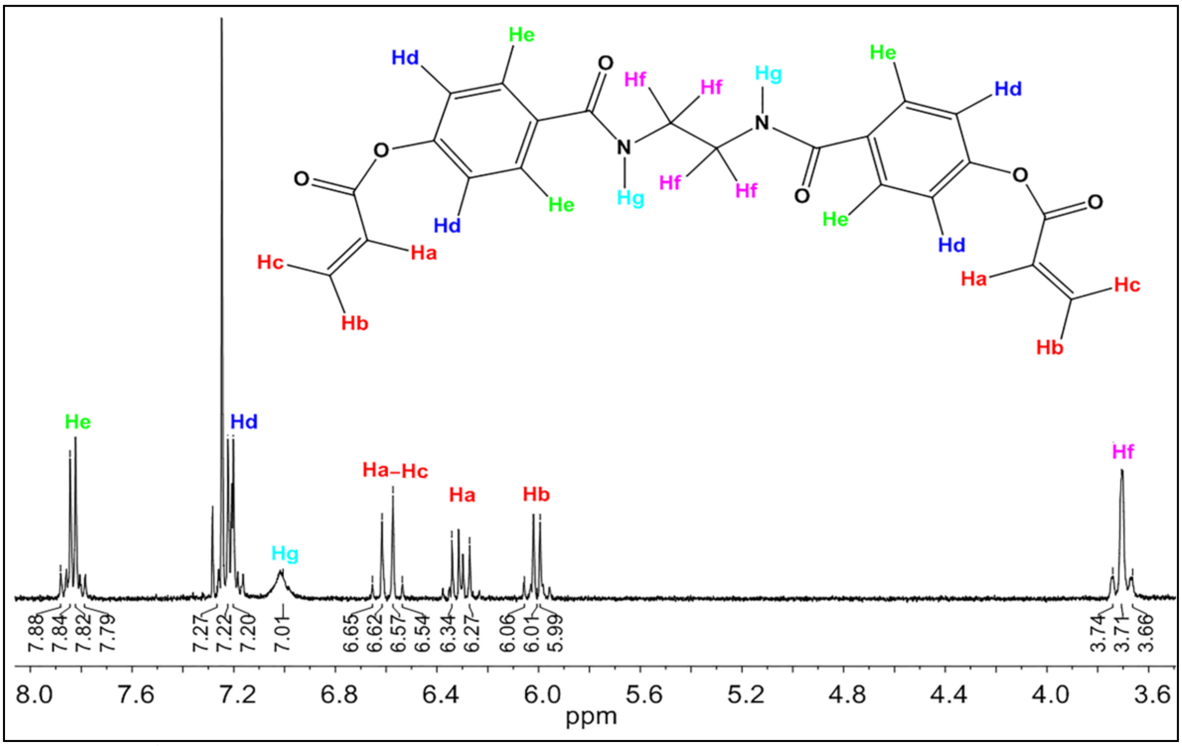

**Fig. 3.** The $^1$H-NMR spectrum of ABCEDA

DSC spectrum of ABCEDA compound was illustrated in Figure 4. The results obtained from DSC measurement, the melting point of ABCEDA was found be about 335°C under $N_2$ atmosphere with heating rate of 10°C /min. Additionally, the exotherm detected at about 246°C may be attributed to transition temperature from amorphous to crystalline form, which is known as the crystallization temperature (Tc).

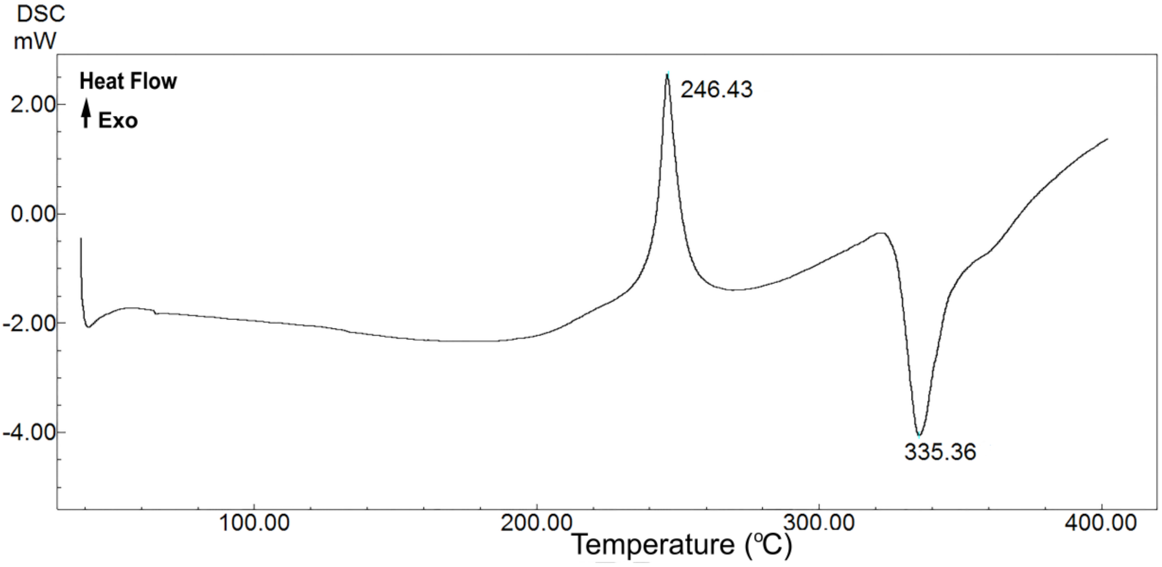

**Fig. 4.** DSC thermogram of ABCEDA

## 3.2. Theoretical characterization of ABCEDA

The optimized molecular structure, bond angle and bond lengths, HOMO, LUMO, electronegativity, chemical hardness, softness, electrophilic index, electrostatic potential were analyzed meticulously to identify the title compound, ((ethane-1,2-diylbis(azanediyl))bis (carbonyl))bis(4,1-phenylene) diacrylate.

### 3.2.1. Molecular geometry

The optimized spatial molecular structure of ABCEDA molecule at minimum energy level were determined theoretically by calculating and the structure having certain numbers for atoms was depicted in Figure 5. The gray, white, red and blue balls in figure symbolized the carbon, hydrogen, oxygen and nitrogen atoms, respectively.

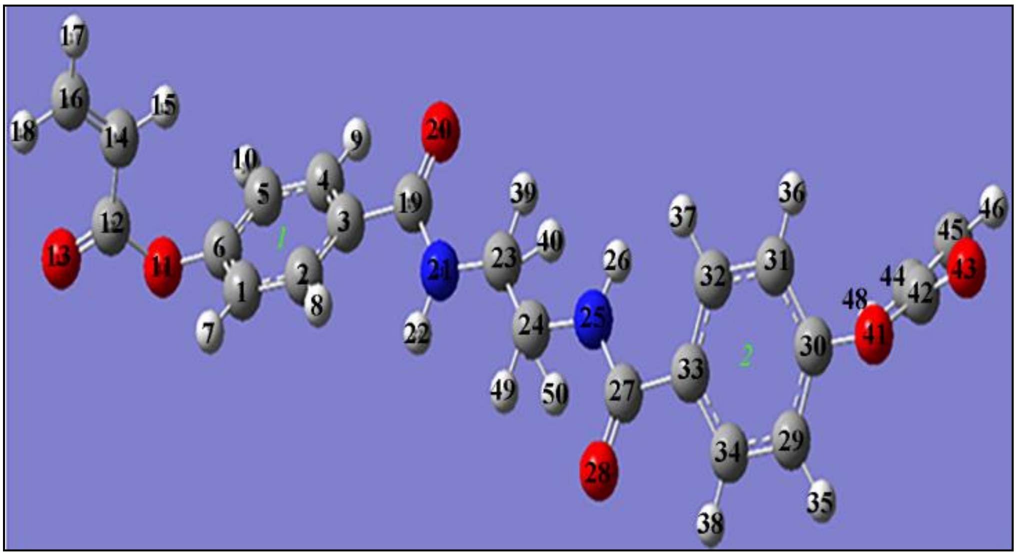

**Fig. 5.** The optimized molecular structure of ABCEDA molecule

The selected geometric characteristics (bond lengths and bond angles) of the title compound, which determining both DFT and HF basis set methods, were depicted in Table 1 and 2, respectively. It was visible from the table that the findings obtained from the DFT and HF methods at 6–31G(d,p) calculation level showed good agreement with each other. However, it was seen to be that the bond angles calculated from DFT method were slightly greater than the results obtained from the HF method. This was caused from taking into account the electron correlation coefficients in DFT calculation method. Thus, DFT method gives more accurate results comparing to HF method. Moreover, the small deviations were detected due to the different distribution of the charge on the atomic bonds in the symmetries of the benzene ring (regular hexagon) existing in "((ethane-1,2-diylbis (azanediyl))bis (carbonyl))bis (4,1phenylene) diacrylate" molecule. In accordance with that, the carbon-carbon double bond distances in the benzene ring-1 was not found to be equal each other. The bond distances for $C_1=C_2$ and $C_1=C_6$ were calculated to be about 1.3839 Å and 1.3826 Å, respectively. This may be significantly originated from the existence of the substituent bonded at different positions and the conjugative effects in the rings (Subashchandrabose et al., 2012). Furthermore, it is clear that the major deviations between the calculated bond lengths were found to be at $C_{12}$-$O_{13}$, $C_{19}$-$O_{20}$, $N_{25}$-$C_{27}$, $C_{27}$-$O_{28}$ and $C_{42}$-$O_{43}$ bonds; 1.1816 Å, 1.2012 Å, 1.3597 Å,1.2009 Å and 1.1815 Å in (B3LYP/6–31G(d,p) method, and 1.1679 Å, 1.1745 Å, 1.3354 Å, 1.1792 Å and 1.1683Å in HF/6–31G(d,p) method, respectively. However, the absence of such a large difference between the bond lengths at $C_6$-$O_{11}$, $O_{11}$-$C_{12}$, $O_{41}$-$C_{42}$ and $C_{30}$-$O_{41}$ caused from the binding of atoms to the nearest carbon atoms with a single bond. Moreover, the C-C bond lengths in the molecule calculated to be between 1.3198-1.4993 Å and 1.3159-1.4922 Å with DFT and HF methods, respectively. Additionally, according to results obtained from B3LYP/6–31G(d,p) methods, $C_{12}$=$O_{13}$, $C_{19}$=$O_{20}$, $C_{27}$=$O_{28}$, $C_{42}$=$O_{43}$ bond distances were computed to be 1.1816, 1.2012, 1.2009 and 1.1815 Å. These observed variations at C=O bonds stemmed from the strong intra-molecular charge transfer (ICT) in the current studied molecule (Qian et al., 2009). Furthermore, the C-O bond lenghts in the present molecule were recorded as 1.3508 ($C_{12}$-$O_{11}$) and 1.3683 Å ($C_{42}$-$C_{41}$) with the same basic set. This results confirm that C-O single bond length is larger than C=O bond (Tezer and Karakus, 2009).

**Table 1.** Theoretically calculated bond lengths (Å) of the title compound

| | **Bond Lenghts (Å)** | |
|---|---|---|
| **Atoms** | **B3LYP/6–31G(d,p)** | **HF/6–31G(d,p)** |
| $C_1$-$C_2$ | 1.3839 | 1.3725 |
| $C_1$-$C_6$ | 1.3826 | 1.3707 |
| $C_1$-$H_7$ | 1.0745 | 1.0694 |
| $C_2$-$H_8$ | 1.0751 | 1.0716 |
| $C_6$-$O_{11}$ | 1.3683 | 1.3597 |
| $O_{11}$-$C_{12}$ | 1.3508 | 1.3488 |
| $C_{12}$-$O_{13}$ | 1.1816 | 1.1679 |
| $C_{12}$-$C_{14}$ | 1.4893 | 1.4867 |
| $C_{14}$-$H_{15}$ | 1.0724 | 1.0677 |
| $C_{14}$-$C_{16}$ | 1.3198 | 1.3159 |
| $C_{19}$-$N_{21}$ | 1.3594 | 1.3512 |
| $C_{19}$-$O_{20}$ | 1.2012 | 1.1745 |
| $C_{27}$-$O_{28}$ | 1.2009 | 1.1792 |
| $N_{21}$-$H_{22}$ | 0.9924 | 0.9897 |
| $N_{25}$-$H_{26}$ | 0.9922 | 0.9895 |
| $N_{21}$-$C_{23}$ | 0.9924 | 0.9897 |
| $C_{30}$-$O_{41}$ | 1.3682 | 1.3599 |
| $C_{27}$-$C_{33}$ | 1.4993 | 1.4876 |
| $C_{34}$-$H_{38}$ | 1.0745 | 1.0694 |
| $C_{44}$-$H_{46}$ | 1.0745 | 1.0694 |
| $C_{44}$-$C_{45}$ | 1.4993 | 1.4922 |
| $C_{42}$-$O_{43}$ | 1.1815 | 1.1683 |
| $C_{45}$-$H_{47}$ | 1.0750 | 1.0678 |
| $N_{25}$-$C_{27}$ | 1.3597 | 1.3354 |
| $O_{41}$-$C_{42}$ | 1.3683 | 1.3598 |
| $C_{42}$-$C_{44}$ | 1.4895 | 1.4856 |

As for the bond angles selected, the larger differences between the findings calculated from DFT and HF basis set methods were noted at the bond angles of $C_{26}$-$N_{25}$-$C_{27}$ and $O_{28}$-$C_{27}$-$N_{25}$ since largest electron density existed on these atoms. This may be attributed to the fact that the DFT method take into account the effect of electron correlation. Moreover, it was visible that there existed the variation in the bond angles at ring-1, and the theoretically calculated bond angles for $C_2$-$C_1$-$C_6$ and $C_1$-$C_2$-$C_3$ were designated as 119.2289° and 120.6328°, respectively. This may be caused from the little distortion in the regular hexagonal symmetry of the phenyl ring, which stemmed from the irregular charge distributions on carbon atoms in the title molecule structure (Hiremath, Kalkoti, and Aralakkanavar, 2009). Moreover, the $O_{11}$-$C_{12}$-$C_{14}$ and $C_3$-$C_{19}$-$N_{21}$ bond angles were noted to be 117.6277° and 116.1840°, respectively. This deviation was directly related to the presence of the strong intra-molecular charge transfer in the synthesized molecules since the vinylic group possessed smaller electronic donor ability than that benzene ring had (Ma et al., 2012). On the other hand, the bond angle of $C_{42}$-$C_{44}$-$C_{45}$ in the vinylic groups of the title molecule was found to be 119.5046°, whereas the bond angle of $C_2$-$C_1$-$H_7$ in the benzene ring was calculated to be about 120.9387°.

**Table 2.** Theoretically calculated bond angles (°) of the title compound

| | **Bond Angles (°)** | |
|---|---|---|
| **Atoms** | **B3LYP/6–31G(d,p)** | **HF/6–31G(d,p)** |
| $C_2$-$C_1$-$C_6$ | 119.2289 | 119.0623 |
| $C_2$-$C_1$-$H_7$ | 120.9387 | 121.1254 |
| $C_1$-$C_2$-$C_3$ | 120.6328 | 121.6507 |
| $C_2$-$C_3$-$C_{19}$ | 123.3936 | 123.0589 |
| $C_1$- $C_6$-$O_{11}$ | 118.7604 | 119.0752 |
| $C_6$-$O_{11}$-$C_{12}$ | 124.1858 | 124.3876 |
| $O_{11}$-$C_{12}$-$O_{13}$ | 118.3830 | 118.6941 |
| $O_{11}$-$C_{12}$-$C_{14}$ | 117.6277 | 117.1126 |
| $H_{17}$-$C_{16}$-$H_{18}$ | 117.9424 | 117.5532 |
| $C_3$-$C_{19}$-$N_{21}$ | 116.1840 | 115.7221 |
| $O_{20}$-$C_{19}$-$N_{21}$ | 122.3814 | 123.0127 |
| $C_{24}$-$N_{25}$-$C_{26}$ | 118.1799 | 119.1006 |
| $C_{26}$-$N_{25}$-$C_{27}$ | 119.1306 | 120.9274 |
| $O_{28}$-$C_{27}$-$N_{25}$ | 122.2913 | 124.4531 |
| $O_{28}$-$C_{27}$-$C_{33}$ | 121.4411 | 121.8098 |
| $O_{41}$-$C_{42}$-$O_{43}$ | 118.4958 | 119.0003 |
| $C_{30}$-$O_{41}$-$C_{42}$ | 124.0540 | 124.9594 |
| $C_{29}$-$C_{30}$-$C_{31}$ | 121.0101 | 122.1656 |
| $O_{43}$-$C_{42}$-$C_{44}$ | 123.9509 | 124.4461 |
| $O_{41}$-$C_{42}$- $C_{44}$ | 117.5251 | 117.9123 |
| $C_{42}$-$C_{44}$-$C_{45}$ | 119.5046 | 120.3377 |
| $H_{46}$-$C_{45}$-$H_{47}$ | 117.9260 | 118.5223 |
| $C_{44}$-$C_{45}$-$H_{46}$ | 120.8999 | 122.0012 |

### 3.2.2. Electrochemical properties of ABCEDA

In this part, the electrochemical and optical characteristics of the title organic compound were investigated in detail. As known, highest occupied molecular orbital (HOMO) and lowest unoccupied molecular orbital (LUMO) allows us to discuss the chemical reaction potential, electrochemical features as well as optical properties and UV-Vis spectra of a molecule (Prasad et al., 2010). HOMO and LUMO also play an important role in interpreting the interaction of the species with each other. HOMO stands for the outermost orbital with the tendency to donate electrons (electron donor), while LUMO is related to innermost orbital having empty place to accept electrons (electron acceptor) (Cakir et al., 2014). In other words, HOMO energy level is associated with the ionization potential, while LUMO directly ascribes the electron affinity. That is, the energy band gap between HOMO and LUMO orbitals gives the information about the stability of the molecule structures. Moreover, the molecular orbital theory states that the $\pi - \pi^*$ transition arises from the interactions of HOMO-LUMO orbitals (Buyukuslu et al, 2010). 3D plots of the he frontier orbitals (HOMOs and LUMOs) of the title compound was depicted in Figure 6. The green blobs showed the negative phase, while the red blobs depicted the positive phase. As seen from the figure, HOMOs and LUMOs were ascribed to predominantly $\pi$-anti-bonding type orbitals. The delocalization of the former orbitals appeared on mostly vicinity of the benzene rings, carbonyl, vinylic and amino groups, but there existed no transition on hydrogen atoms in the molecule. Large delocalization of charge density came into view over the molecule, which may be caused from that the molecule possessed mainly planar structure and acted softly as electrophilic (Hatch et al, 2000). The another crucial parameter deduced from the HOMO-LUMO orbitals was optical band gap energy indicating the kinetic stability and chemical reactivity of the molecule (Lewis et al, 1994). Namely, the increasing of optical band gap caused the decrement in the reactivity (mainly polarizability) and increment in the stability of the structure. So, a compound with low kinetic stability and high chemical reactivity is defined as soft materials (Cakir et al., 2014). As for the title compound, HOMO and LUMO energy values was computed to be about -0.3105 a.u. (-8.4491 eV) and 0.0799 a.u (2.1742 eV) for the synthesized molecule at B3LYP/6-31G(d,p) calculation level, respectively. The energy difference between HOMO and LUMO (optical band gap energy) was found to be 0.3904 (10.6233 eV) a.u. This result show that the title molecule had quite stability (Ozdemir et al, 2010). Correspondingly, the calculated HOMO and LUMO Eigen values (5.2913 and -20.6264 a.u., respectively) showed that the studied compound had relatively low electronic donor ability, polarizability and chemical reactivity (Bakhshi and Rattan, 1998).

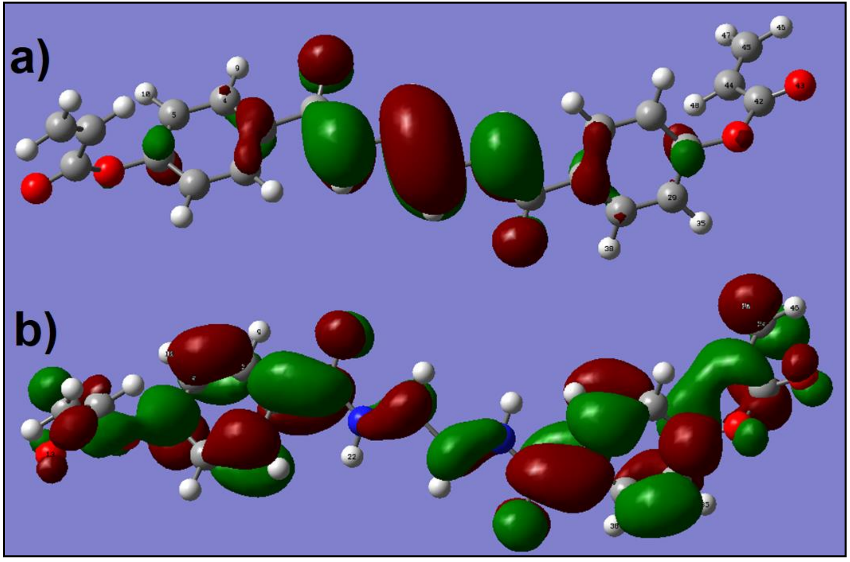

**Fig. 6.** 3D maps of the a) LUMO and b) HOMO of ABCEDA

At time same time, the electronegativity (χ), chemical hardness (η), electrophilic index (ψ) and softness (ζ ) quantities determined by using the electron affinity and ionization potential values were computed with the use of HOMO-LUMO energies of the synthesized molecule. The obtained data were tabulated in Table 3. According to the table, χ and ψ values of the title compounds were calculated to be about 0.1153 a.u. (3.1375 eV) and 0.0052 a.u. (0.1415 eV), respectively. This result was attributed the fact that the studied compound mostly possessed the possible active sites condensing on oxygen atoms for electrophilic attack (supported by MEP analyses). Furthermore, η value of the molecule was found to be about 0.1952 a.u. (5.3117 eV), whereas ζ value is computed to be about 2.5336 a.u. (68.9428 eV), which illustrating the title compound may be used for the optic and optoelectronic applications (Koca et al, 2012)

**Table 3.** Calculated energy values in the ground state at B3LYP/6-31G(d,p) level of theory

| **Quantity** | **Value (a.u.)** | **Value (eV)** |
|---|---|---|
| Lowest Molecular Orbital Eigen Value | -20.6264 | -561.2730 |
| Highest Molecular Orbital Eigen Value | 5.2913 | 143.9837 |
| HOMO | -0.3105 | -8.4491 |
| LUMO | 0.0799 | 2.1742 |
| HOMO–LUMO, optical band gap energy, $\lvert \Delta E \rvert$ | 0.3905 | 10.6261 |
| χ (electronegativity) | 0.1153 | 3.1375 |
| η (chemical hardness) | 0.1952 | 5.3117 |
| ψ (electrophilic index) | 0.0052 | 0.1415 |
| ζ $(\text{softness})^{-1}$ | 2.5336 | 68.9428 |

### 3.2.3. Molecular electrostatic potential and electrostatic potential analyses

Molecular electrostatic potential (MEP) and electrostatic potential (ESP) are the significant properties to depict the charge distribution of a molecule. The useful information about the interaction of the molecule with another molecules is obtained from 3D maps of both MEP and ESP. The molecular electrostatic potential *V(r)* can be defined as the interaction energy between the electrical charge produced from the nuclei and electrons of the title molecule and a proton (a positive test charge) located at the certain point, r (*x*, *y*, *z*)(Ozdemir et al., 2010; Soykan et al., 2013). As depending on electronic density, MEP indicates the sites presenting in the molecule for electrophilic reactions, nucleophilic attacks and also the hydrogen bond interactions (Parlak et al., 2011). The 3D map of the MEP belonging to the title molecule was depicted in the Figure 7. Herein, the nucleophilic reactivity, electrophilic reactivity and non-reactive sites on the studied molecule were presented by blue (positive), red(negative) and green/yellow (notr) regions, respectively. It is visible from the figure that there existed four possible electrophilic sites on the molecule for the intermolecular interactions. The most negative regions meaning the existence of excess negative charge were delocalized on the carbonly groups and oxygen atoms on the studied compound. On the other hand, it was obvious from the figure that the nucleophilic reactivity of the title compound was localized on the hydrogen atoms and vinylic groups. That is, the studied molecule possessed possible reactivity for the interaction intermolecularly and metallically. Moreover, the title molecule with the nucleophilic reactivity caused from two terminally locating vinylic groups may be useful for the cross-linking reaction. Moreover, the electrostatic potential (ESP) image belonging to ABCEDA molecule was depicted in the Figure 8. Here, negative ESP was presented as the yellowish blob whereas negative ESP reflected as the reddish blob. As known, ESP is related to the electronegativity on an atom and the partial charge distribution in a molecule. It was apparent from the image, the most negative ESP spread over mainly on the oxygen atoms existing in the structure. This showed that π-electrons delocalized over the carbonyl groups and at the junctions of vinylic and benzene rings with these carbonyl groups in the molecule. On the other hand, it was visible from the figure that the positive ESP spread over the rest of the studied molecule.

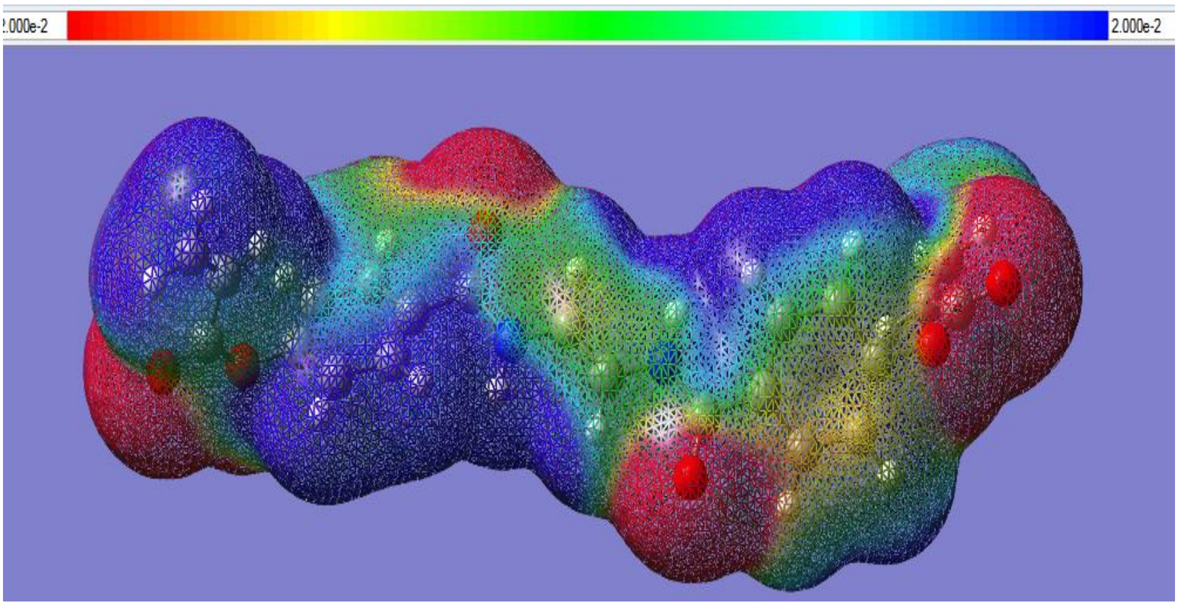

**Fig. 7.** 3D map of the molecular electrostatic potential (MEP) of the ABCEDA molecule

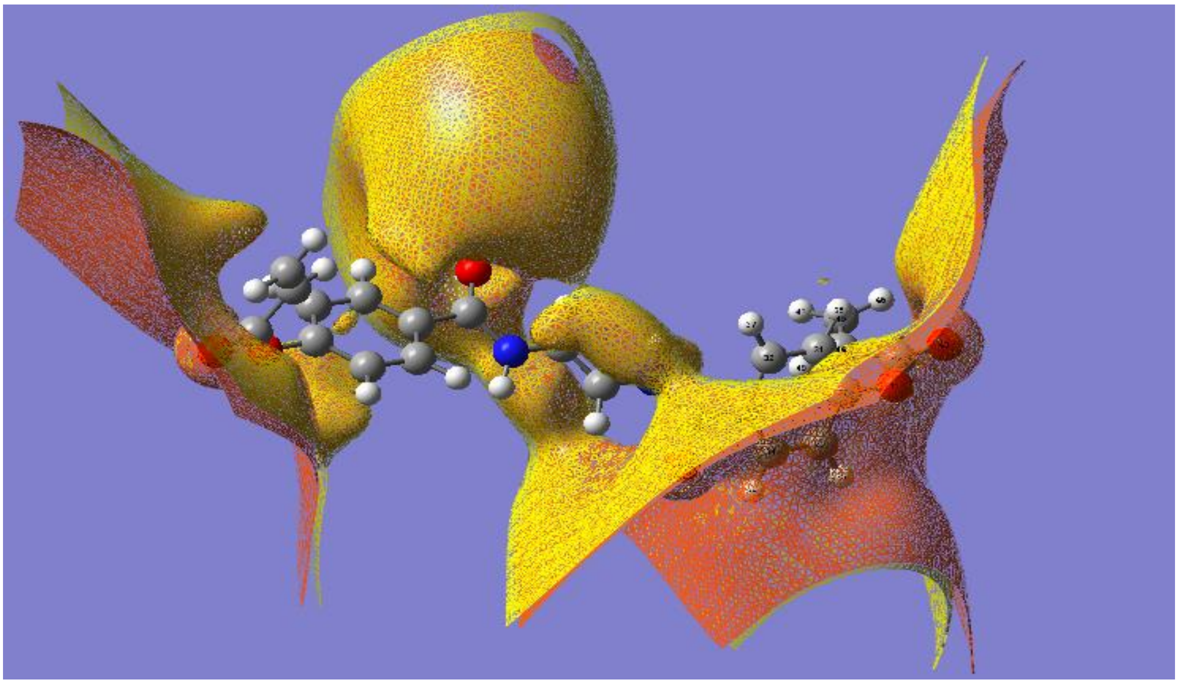

**Fig. 8.** 3D map of the electrostatic potential (ESP) of ABCEDA molecule

## 4. Conclusion

In this multidisciplinary study, we not only synthesize the novel ((ethane-1,2-diylbis (azanediyl))bis(carbonyl))bis (4,1-phenylene) diacrylate (ABCEDA) molecule but also characterize both experimentally by means of FTIR, DSC and $^1$H-NMR tecniques and theoretically by using density functional theory (DFT) and Hartree Fock (HF) method for the first time. The synthesis of ABCEDA molecules was performed with the three reaction steps and the yield was found to be 68 wt%. As a result of this study, the following major finding were concluded:

- ✓ The characteristic absorption bands belonging to amide, ester, phenyl and vinylic groups in the title molecule and the characteristic peaks obtained from the $^1$H-NMR spectrum showed good correlation with the molecular structure of the ABCEDA compound.
- ✓ The melting temperature of the title molecule was obtained to be about 335°C in the DSC spectrum. There was also exotherm at 246°C attributing to the crystallization temperature (transition temperature from amorphous to crystalline form).
- ✓ The most optimized spatial molecular structure of ABCEDA molecule at minimum energy level were determined with the aid of theoretical calculation. Moreover, the molecular geometry properties (bond angles and bond lengths) of the molecule were computed by both DFT and HF method. The obtained results revealed that there existed some little deviations on the bond angles and bond lengths of the molecule due to the difference in the nature of the applied calculation methods.
- ✓ As for electrochemical properties of ABCEDA, HOMOs and LUMOs of the title compound were ascribed to predominantly $\pi$-antibonding-type orbitals. The delocalizations were seen mainly on vicinity of the benzene rings, carbonyl, vinylic and amino groups. Furthermore, the theoretical findings showed that the molecule possessed mainly planar structure and acted softly as electrophilic. Additionally, the novel compound was found to be soft material due to having the low kinetic stability and high chemical reactivity.
- ✓ MEP map presented that the title molecule had the nucleophilic and electrophilic reactive sites. The negative regions were delocalized on the carbonly groups and oxygen atoms, while the positive regions were localized on the hydrogen atoms and vinylic groups. Moreover, it was apparent from ESP, the most negative ESP spread over mainly on the oxygen atoms in the title compound studied.

## Acknowledgments

This work was supported by BAIBU research fund grand no. BAP-2014.03.03.686. Furthermore, the authors especially thanks to Scientific, Industrial and Technological application and Research Center (BETUM) and Innovative Food Technologies Development Application and Research Center (YENIGIDAM) for valuable supports.

## References

Abdelkader, A. F., White, J. R., 2005. Curing Characteristics and Internal Stresses in Epoxy Coatings: Effect of Crosslinking Agent. Journal of Materials Science, 40(8): 1843-1854.

Akyildiz, F., Alyar, S., Bilkan, M. T., Alyar, H., 2018. Synthesis, Characterization, Spectroscopic Properties, DFT Calculations and Antimicrobial Activities of p-toluenesulfonamide,N,N'-1,3-propanediylbis(ptspr) and [Cu(II)(phenanthroline) (2)]ptspr. Journal of Molecular Structure, 1174: 160-170.

Arioglu, C., Tamer, O., Avci, D., Atalay, Y., 2018. Optimized Geometry, Spectroscopic Characterization and Nonlinear Optical Properties of Carbazole Picrate: A Density Functional Theory Study. Indian Journal of Physics, 92(12): 1613-1621.

Bakhshi, A. K., Rattan, P., 1998. Ab Initio Study of Novel Low-Band-Gap Donor-Acceptor Polymers Based on Poly (Cyclopentadienylene). Journal of the Chemical Society-Faraday Transactions, 94(18): 2823-2826.

Benhamou, M., Chahid, M., 2008. Field-Theoretical Renormalization-Group Approach to Critical Dynamics of Crosslinked Polymer Blends. European Physical Journal E, 27(1): 57-62.

Benmouna, F., Maschke, U., Coqueret, X., Benmouna, M., 2001. Theoretical Phase Behavior of Crosslinked Polymers and Liquid Crystals. Macromolecular Theory and Simulations, 10(1): 63-70.

Buyukuslu, H., Akdogan, M., Yildirim, G., Parlak, C., 2010. Ab Initio Hartree-Fock and Density Functional Theory Study on Characterization of 3-(5-methylthiazol-2-yldiazenyl)-2-phenyl-1H-indole. Spectrochimica Acta Part a-Molecular and Biomolecular Spectroscopy, 75(4): 1362-1369.

Cakir, I., Soykan, U., Cetin, S., Karaboga, F., Zalaoglu, Y., Dogruer, M., Terzioglu, C., Yildirim, G., 2014. Electrochemical and Spectroscopic Characteristics of p-Acryloyloxybenzoyl Chloride and p-Acryloyloxybenzoic Acid and Antimicrobial Activity of Organic Compounds. Spectrochimica Acta Part a-Molecular and Biomolecular Spectroscopy, 132: 502-513.

Ceylan, U., Tari, G. O., Gokce, H., Agar, E., 2016. Spectroscopic (FT-IR and UV-Vis) and Theoretical (HF and DFT) Investigation of 2-Ethyl-N-[(5-nitrothiophene-2-yl) methylidene] Aniline. Journal of Molecular Structure, 1110: 1-10.

Cirak, C., Koc, N., 2012. Molecular Structure and Effects of Intermolecular Hydrogen Bonding on the Vibrational Spectrum of Trifluorothymine, an Antitumor and Antiviral Agent. Journal of Molecular Modeling, 18(9): 4453-4464.

Cormack, P. A. G., Elorza, A. Z., 2004. Molecularly Imprinted Polymers: Synthesis and Characterisation. Journal of Chromatography B-Analytical Technologies in the Biomedical and Life Sciences, 804(1): 173-182.

Durig, J. R., El-Defrawy, A. M., Ganguly, A., Panikar, S. S., Soliman, M. S., 2011. Conformational Stability from Variable-Temperature Infrared Spectra of Xenon Solutions, r(0) Structural Parameters, and Vibrational Assignment of Pyrrolidine. Journal of Physical Chemistry A, 115(26): 7473-7483.

Elder, B. D., Mohan, A., Athanasiou, K. A., 2011. Beneficial Effects of Exogenous Crosslinking Agents on Self-Assembled Tissue Engineered Cartilage Construct Biomechanical Properties. Journal of Mechanics in Medicine and Biology, 11(2): 433-443.

Gao, C., Yan, T., Dai, K. R., Wan, Y. Z., 2012. Immobilization of Gelatin onto Natural Nanofibers for Tissue Engineering Scaffold Applications without Utilization of any Crosslinking Agent. Cellulose, 19(3): 761-768.

Gokce, H., Bahceli, S., 2011. A Study on Quantum Chemical Calculations of 3-, 4-nitrobenzaldehyde Oximes. Spectrochimica Acta Part a-Molecular and Biomolecular Spectroscopy, 79(5): 1783-1793.

Gomez, C. G., Strumia, M. C., 2001. Synthesis of a Triacrylate Crosslinking Agent and Its Use in the Preparation of Macroporous Polymers. Polymer Bulletin, 47(3-4): 261-268.

Hatch, F. T., Lightstone, F. C., Colvin, M. E., 2000. Quantitative Structure-Activity Relationship of Flavonoids for Inhibition of Heterocyclic Amine Mutagenicity. Environmental and Molecular Mutagenesis, 35(4): 279-299.

Hiremath, C. S., Kalkoti, G. B., Aralakkanavar, M. K., 2009. Revised Vibrational Band Assignments for the Experimental IR and Raman Spectra of 2,3,4-Trifluorobenzonitrile Based on ab Initio, DFT and Normal Coordinate Calculations. Spectrochimica Acta Part a-Molecular and Biomolecular Spectroscopy, 74(1): 200-204.

Iwakura, C., Furukawa, N., Ohnishi, T., Sakamoto, K., Nohara, S., Inoue, H., 2001. Nickel/Metal Hydride Cells Using an Alkaline Polymer Gel Electrolyte Based on Potassium Salt of Crosslinked Poly (Acrylic Acid). Electrochemistry, 69(9): 659-663.

Karaboga, F., Soykan, U., Dogruer, M., Ozturk, B., Yildirim, G., Cetin, S., Terzioglu, C., 2013. Experimental and Theoretical Approaches for Identification of p-Benzophenoneoxycarbonylphenyl Acrylate. Spectrochimica Acta Part a-Molecular and Biomolecular Spectroscopy, 113: 80-91.

Koca, M., Yildirim, G., Kirilmis, C., Karaboga, F., 2012. Density Functional Theory Study on the Identification of Pd(Me-Xanthate)(2). Arabian Journal for Science and Engineering, 37(5): 1283-1291.

Lenhart, J. L., Cole, P. J., 2006. Adhesion Properties of Lightly Crosslinked Solvent-Swollen Polymer Gels. Journal of Adhesion, 82(10): 945-971.

Lewis, D. F. V., Ioannides, C., Parke, D. V., 1994. Interaction of a Series of Nitriles with the Alcohol-Inducible Isoform of P450 - Computer-Analysis of Structure-Activity-Relationships. Xenobiotica, 24(5): 401-408.

Luo, D., Li, Y., Yang, M. J., 2011. Preparation and Characterization of Novel Crosslinked Poly[glycidyl methacrylate-poly(ethylene glycol) methyl ether methacrylate] as Gel Polymer Electrolytes. Journal of Applied Polymer Science, 120(5): 2979-2984.

Ma, X., Jiao, J. M., Yang, J., Huang, X. B., Cheng, Y. X., Zhu, C. J., 2012. Large Stokes Shift Chiral Polymers Containing (R,R)-Salen-Based Binuclear Boron Complex: Synthesis, Characterization, and Fluorescence properties. Polymer, 53(18): 3894-3899.

Margel, S., Nov, E., Fisher, I., 1991. Polychloromethylstyrene Microspheres - Synthesis and Characterization. Journal of Polymer Science Part a-Polymer Chemistry, 29(3): 347-355.

Martinez, A., Blanco, M. D., Davidenko, N., Cameron, R. E., 2015. Tailoring Chitosan/Collagen Scaffolds for Tissue Engineering: Effect of Composition and Different Crosslinking Agents on Scaffold Properties. Carbohydrate Polymers, 132: 606-619.

Maryanski, M. J., Audet, C., Gore, J. C., 1997. Effects of Crosslinking and Temperature on the Dose Response of a BANG Polymer Gel Dosimeter. Physics in Medicine and Biology, 42(2): 303-311.

Montazer, M., Jolaei, M. M., 2010. beta-Cyclodextrin Stabilized on Three-Dimensional Polyester Fabric with Different Crosslinking Agents. Journal of Applied Polymer Science, 116(1): 210-217.

Osada, Y., Gong, J. P., Tanaka, Y., 2004. Polymer Gels (Reprinted from Functional Monomers and Polymers, pg 497-528, 1997). Journal of Macromolecular Science-Polymer Reviews, C44(1): 87-112.

Ozdemir, N., Eren, B., Dincer, M., Bekdemir, Y., 2010. Experimental and ab Initio Computational Studies on 4-(1H-benzo[d]imidazol-2-yl)-N,N-dimethylaniline. Molecular Physics, 108(1): 13-24.

Park, K. Y., Jeong, W. W., Suh, K. D., 2003. Monodisperse Crosslinked Microsphere Polymer Particles by Dispersion Copolymerization of Glycidyl Methacrylate and Divinylbenzene. Journal of Macromolecular Science-Pure and Applied Chemistry, A40(6): 617-627.

Parlak, C., Akdogan, M., Yildirim, G., Karagoz, N., Budak, E., Terzioglu, C., 2011. Density Functional Theory Study on the Identification of 3-[(2-morpholinoethylimino)methyl]benzene-1,2-diol. Spectrochimica Acta Part a-Molecular and Biomolecular Spectroscopy, 79(1): 263-271.

Pascal, J. A., Medidhi, K. R., Oyanader, M. A., Stretz, H. A., Arce, P. E., 2019. Understanding Collaborative Effects between the Polymer Gel Structure and the Applied Electrical Field in Gel Electrophoresis Separation. International Journal of Polymer Science, 2019: Article ID 6194674, 15 pages.

Philip, C. M., Mathew, B., 2008. Design of EGDMA-Crosslinked Theophylline Imprinted Polymer with High Specificity and Selectivity. Journal of Macromolecular Science Part a-Pure and Applied Chemistry, 45(4): 335-343.

Pittman, C. U., Xu, X. M., Wang, L. C., Toghiani, H., 2000. Mechanical and Viscoelastic Properties of Semi-Interpenetrating Polymer Networks of Poly (Vinyl Chloride)/Thermosetting Resin Blends. Polymer Engineering and Science, 40(6): 1405-1413.

Prasad, O., Sinha, L., Misra, N., Narayan, V., Kumar, N., Pathak, J., 2010. Molecular Structure and Vibrational Study on 2,3-dihydro-1H-indene and Its Derivative 1H-indene-1,3(2H)-dione by Density Functional Theory Calculations. Journal of Molecular Structure-Theochem, 940(1-3): 82-86.

Qian, G., Zhong, Z., Luo, M., Yu, D., Zhang, Z., Ma, D., Wang, Z. Y., 2009. Synthesis and Application of Thiadiazoloquinoxaline-Containing Chromophores as Dopants for Efficient Near-Infrared Organic Light-Emitting Diodes. Journal of Physical Chemistry C, 113(4): 1589-1595.

Sert, Y., Gokce, H., Chandra, Mahendra, M., Srikantamurthy, N., Cirak, C., 2019. Molecular Docking and Vibrational Spectroscopy Studies of (E)-N '-hydroxy-1,3-diphenyl-4,5-dihydro-1H-pyrazole-5-Carboximidamide. Journal of Molecular Structure, 1184: 79-91.

Smolin, Y. Y., Janakiraman, S., Soroush, M., Lau, K. K. S., 2017. Experimental and Theoretical Investigation of Dye Sensitized Solar Cells Integrated with Crosslinked Poly (Vinylpyrrolidone) Polymer Electrolyte Using Initiated Chemical Vapor Deposition. Thin Solid Films, 635: 9-16.

Soykan, U., Cetin, S., Ozturk, B., Karaboga, F., Zalaoglu, Y., Dogruer, M., Terzioglu, C., 2013. Synthesis and Characterization of p-Benzophenoneoxycarbonylphenyl Acrylate by Means of Experimental Measurements and Theoretical Approaches, and Bulk Melt Polymerization. Journal of Molecular Structure, 1049: 479-487.

Stankova, M., Jandera, P., Hajek, T., 2013. Characterization of Prepared Monilithic Capillary Columns. Chemicke Listy, 107: S449-S451.

Stephens, P. J., Devlin, F. J., Chabalowski, C. F., Frisch, M. J., 1994. Ab-Initio Calculation of Vibrational Absorption and Circular-Dichroism Spectra Using Density-Functional Force-Fields. Journal of Physical Chemistry, 98(45): 11623-11627.

Subashchandrabose, S., Saleem, H., Erdogdu, Y., Dereli, O., Thanikachalam, V., Jayabharathi, J., 2012. Structural, Vibrational and Hyperpolarizability Calculation of (E)-2-(2-hydroxybenzylideneamino)-3-Methylbutanoic Acid. Spectrochimica Acta Part a-Molecular and Biomolecular Spectroscopy, 86: 231-241.

Sun, Y. X., Hao, Q. L., Lu, L. D., Wang, X., Yang, X. J., 2010. Vibrational Spectroscopic Study of o-, m- and p-hydroxybenzylideneaminoantipyrines. Spectrochimica Acta Part a-Molecular and Biomolecular Spectroscopy, 75(1): 203-211.

Tezer, N., Karakus, N. 2009., Theoretical Study on the Ground State Intramolecular Proton Transfer (IPT) and Solvation Effect in Two Schiff Bases Formed by 2-aminopyridine with 2-hydroxy-1-naphthaldehyde and 2-hydroxy salicylaldehyde. Journal of Molecular Modeling, 15(3): 223-232.

Ucun, F., Guclu, V., Saglam, A., 2008. Ab initio Hartree-Fock and Density Functional Theory Study on Molecular Structures, Energies, and Vibrational Frequencies of Conformations of 2-hydroxy-3-nitropyridine and 3-hydroxy-2-nitropyridine. Spectrochimica Acta Part a-Molecular and Biomolecular Spectroscopy, 70(3): 524-531.

Yin, C., Xu, A. H., Gong, L., Zhang, L. Q., Geng, B., Zhang, S. X., 2015. Preparation of Slightly Crosslinked Monodisperse Poly (Maleic Anhydride-Cyclohexyl Vinyl ether-divinylbenzene) Functional Microspheres with Anhydride Groups via Precipitation Polymerization. Particuology, 19: 99-106.

Zhan, X. B., Cai, X. Q., Zhang, J. Y., 2018. A Novel Crosslinking Agent of Polymethyl(ketoxime)siloxane for Room Temperature Vulcanized Silicone Rubbers: Synthesis, Properties and Thermal Stability. Rsc Advances, 8(23): 12517-12525.

Zhang, X. Y., Wang, X. P., Li, L., Zhang, S. S., Wu, R. N., 2015. Preparation and Swelling Behaviors of a High Temperature Resistant Superabsorbent Using Tetraallylammonium Chloride as Crosslinking Agent. Reactive and Functional Polymers, 87: 15-21.

Zhao, X. F., Li, Z. J., Wang, L., Lai, X. J., 2008. Synthesis, Characterization, and Adsorption Capacity of Crosslinked Starch Microspheres with N,N '-methylene Bisacrylamide. Journal of Applied Polymer Science, 109(4): 2571-2575.